High-Responsivity Graphene-on-Silicon Slot Waveguide Photodetectors

Jiaqi Wang[a, †], Zhenzhou Cheng[b, †,*], Zefeng Chen[a], Xi Wan[a], Bingqing Zhu[a], Hon Ki Tsang[a], Chester Shu[a,*], and Jianbin Xu[a]

[a] Department of Electronic Engineering, The Chinese University of Hong Kong, Shatin, N.T., Hong Kong.

[b] Department of Chemistry, The University of Tokyo, Tokyo 113-0033, Japan

[*] Email: ctshu@ee.cuhk.edu.hk , zzcheng@chem.s.u-tokyo.ac.jp

[†] These authors contributed equally to this work.

Electronic Supplementary Information

Fabrication process of the graphene-on-silicon slot waveguide photodetectors

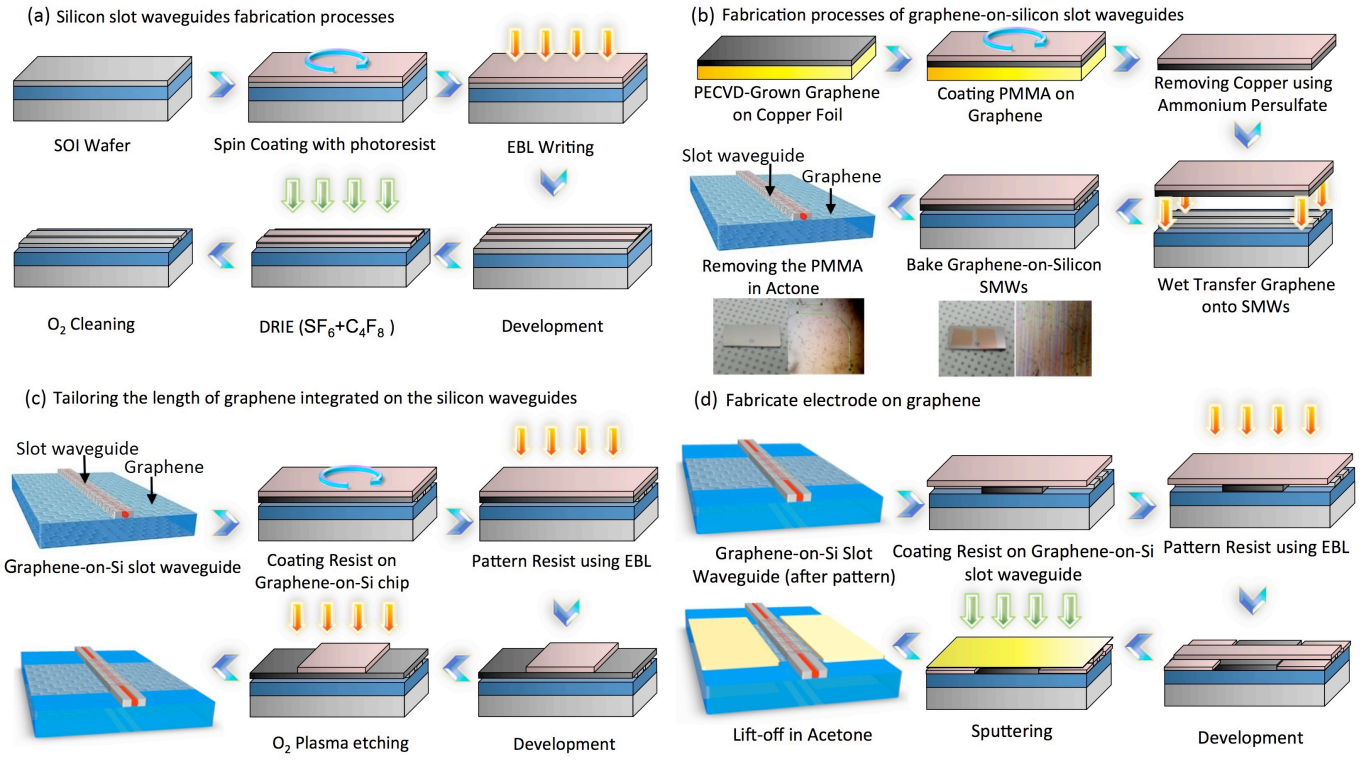

Fig. S1 Fabrication process of the graphene-on-silicon slot waveguide photodetector.

The schematic illustration of the fabrication process of the graphene-on-silicon slot waveguide photodetector is shown in Fig. S1. The silicon devices were fabricated on a commercial silicon-on-insulator (SOI) wafer (SOITEC Inc.) with 250 nm top silicon layer and 3.0 μm buried oxide (BOX). Patterns of silicon devices were defined by using standard electron-beam lithography (EBL) (Elionix ELS 7800) with 80 kV beam voltage and positive electron beam resist ZEP-520A. The grating coupler and waveguide structure were then transferred to the wafer by deep reactive-ion etching (Oxford Plasma Lab 100) with a mixture gas of C_4F_8, SF_6 and Ar.

Next, a commercial chemical vapor deposition (CVD) grown graphene sheet on copper foil (Graphene Laboratories Inc.) was spin-coated with 200nm polymethyl methacrylate (PMMA) layer on top. The copper substrate was then removed by wet etching with ammonium persulfate solution ($(NH_4)_2S_2O_8$ 0.44 mol/L). The graphene supported by PMMA was rinsed by deionized water and transferred onto the silicon chip. After dried in the air, the silicon chip was baked at 150 °C for 15 minutes to soften the PMMA resist, allowing better contact between graphene sheet and the silicon devices. The chip was then baked at 80 °C for 30 minutes on a hotplate to improve adhesion of the graphene sheet to the silicon chip. Next, EBL was applied to define the PMMA mask on the graphene-on-silicon slot waveguide. Oxygen plasma etching (Oxford Plasma Lab 80) was used to remove the graphene area that was exposed. Finally, the PMMA was removed by acetone. Scanning electron microscope (SEM) images of the fabricated graphene-on-silicon slot waveguide devices were shown in Fig. S2 (a), (b). Micro Raman spectroscopy was applied to characterize the monolayer graphene on the slot waveguide. The Raman spectrum, collected with 512 nm excitation, was shown in Fig. S2 (c). The G and 2D peaks were at 1588 cm^{-1} and

2690 cm^{-1}, and the intensity ratio was less than 0.5, indicating a monolayer graphene [S1].

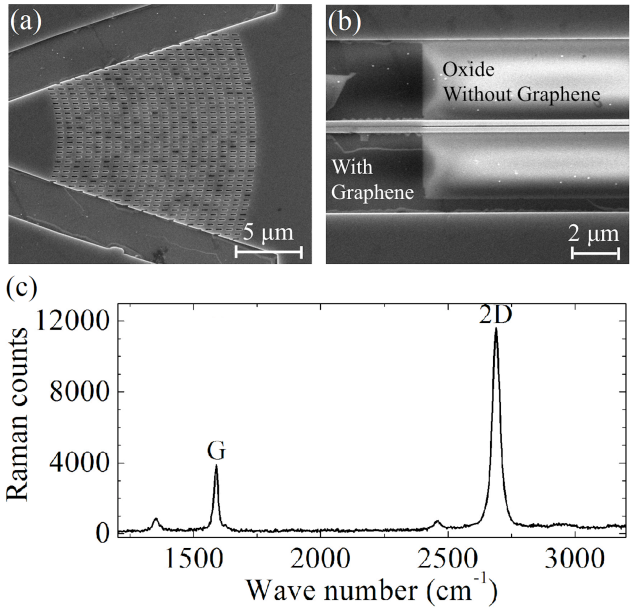

Fig. S2 (a) SEM image of the subwavelength grating. (b) SEM image of the graphene-on-silicon slot waveguide. The area with and without graphene can be clearly identified. (c) Raman spectrum of the graphene integrated on the silicon slot waveguide.

Saturable absorption measurement of the graphene-on-silicon slot waveguide device

Saturable absorption in graphene-on-silicon slot waveguide with 17 μm-long graphene integrated on top was measured with a pulsed laser. The experimental set up was shown in Fig. S3 (a). The pulsed laser source was a home-built gain-switched laser with 50 ps pulse width and 1 MHz repetition rate at a center wavelength of 1555.65 nm. The laser was amplified and the output was subsequently filtered by an optical bandpass filter. The transmission of the graphene-on-silicon slot waveguide as a function of the coupled pulse energy is shown in Fig. S3 (b). At low pulse energy, the transmission is independent of the energy. At high pulse energy, the increased concentration of the excited electrons resulted in band filling and blocked some absorption [S2], leading to a stronger transmission. As shown in Fig. S3 (b), the transmission increased rapidly when the coupled input pulse energy was larger than 20 pJ. When the pulse energy was 0.167 nJ the transmission was 44% larger than the low power regime. The in-plane saturable absorption can be modeled by the two-stage saturable absorption model [S2]

$$\alpha(E) = \frac{\alpha_S}{(1+\frac{E}{E_S})} + \alpha_{NS}$$

where α_S and α_{NS} are the saturable and non-saturable absorption components, E_S is the saturation pulse energy. From curve fitting, the values of α_S, α_{NS} and E_S are obtained as 0.05 μm^{-1}, 0.019 μm^{-1}, and 213 pJ, respectively. The saturation energy was relatively low comparing to the 3.9 nJ [3] in the case of the graphene-on-silicon channel waveguide. The reason is that the optical interaction was significantly enhanced in the graphene-on-slot waveguide configuration. Also, a smaller area of graphene is used on the silicon slot waveguide.

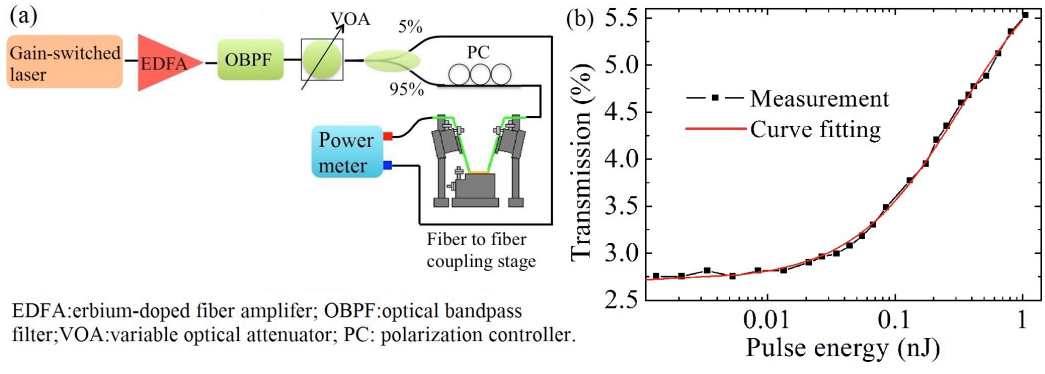

Fig. S3 (a) Schematic of the saturable absorption measurement setup. (b) Saturable absorption measurement of graphene-on-silicon slot waveguide.

Photoresponse measurement of the graphene-on-silicon slot waveguide photodetector

The amplified CW laser (HP 8168F) at 1550 nm was coupled into the waveguide through the grating coupler. The bias voltage was supplied by a Keithley 2400 source meter which also recorded the current. For each chosen optical power, the bias voltage was swept twice, once with (I_{on}) and once without the light (I_{off}). The photocurrent was subtracted from the two measurements (I_{on}-I_{off}). In the dynamic response measurement, the laser was modulated with a 1 kHz 50% duty cycle square wave with a coupled power of 0.5 mW. The bias voltage was 2 V. The photocurrent was then amplified by a current sensitive preamplifer and recorded by a 500 MHz oscilloscope. The recorded waveform was shown in Fig.S4 (a). Fig. S4 (b) shows the enlarged details of the rising ridge of the photocurrent. The rise time of the photodetector was ~50 μs.

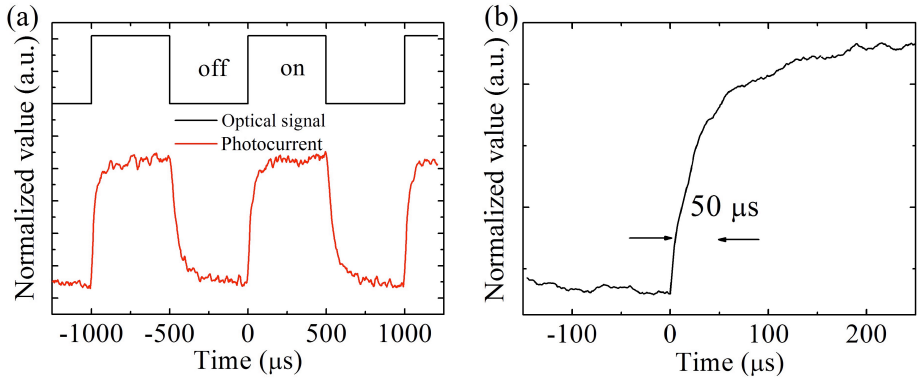

Fig. S4 (a) Dynamic response of the graphene-on-silicon slot waveguide photodetector, with a 1K Hz square wave excitation. (b) The enlarged details of the rising edge of the photocurrent, of which the rise time was ~50 μs.

Reference:

[S1] X. Wang, Z. Cheng, K. Xu, H. K. Tsang, and J. Xu, Nat. Photonics, 2013, **7**, 888-891.

[S2] Z. Sun, T. Hasan, F. Torrisi, D. Popa, G. Privitera, F. Wang, F. Bonaccorso, D. M. Basko and A. C. Ferrari, *ACS Nano,* 2010, **4**, 803-810.

[S3] Z. Shi, C.Y. Wong, Z. Cheng, K. Xu and H. K. Tsang, In Conference on Lasers and Electro-Optics/Pacific Rim, Optical Society of America (2013).